Journal of Statistical Physics, Vol. 59, Nos. 5/6, 1990

Renormalization of Binary Trees Derived from One-Dimensional Unimodal Maps

Yuzhen Ge,[1] Edmond Rusjan,[1] and Paul Zweifel[1]

Received June 12, 1989; revision received January 19, 1990

For one-dimensional unimodal maps $h_\lambda(x): I \to I$, where $I = [x_0, x_1]$ when $\lambda = \lambda_{\max}$, a binary tree which includes all the periodic windows in the chaotic regime is constructed. By associating each element in the tree with the superstable parameter value of the corresponding periodic interval, we define a different unimodal map. After applying a certain renormalization procedure to this new unimodal map, we find the period-doubling fixed point and the scaling constant. The period-doubling fixed point depends on the details of the map $h_\lambda(x)$, whereas the scaling constant equals the derivative $h'_{\lambda_{\max}}(x_0)$. The thermodynamics and the scaling function of the resulting dynamical system are also discussed. In addition, the total measure of the periodic windows is calculated with results in basic agreement with those obtained previously by Farmer. Up to 13 levels of the tree have been included, and the convergence of the partial sums of the measure is shown explicitly. A new scaling law has been observed, i.e., the product of the length of a periodic interval characterized by sequence Q and the scaling constant of Q is found to be approximately 1.

KEY WORDS: Nonlinear dynamics; chaos; one-dimensional unimodal maps; bifurcation; universality; renormalization; scaling; partition function; fixed point; Hausdorff dimension.

1. INTRODUCTION

One of the most important goals of studying chaos is to find universalities. In one-dimensional unimodal maps universalities are well exhibited. For example, the Feigenbaum exponent δ which describes the rate of convergence of bifurcation point toward the accumulation point is universal.[1] Furthermore, applying a renormalization operation to a one-dimensional quadratic map, it is found that this operator has a unique fixed point.

[1] Center for Transport Theory and Mathematical Physics, Virginia Polytechnic Institute and State University, Blacksburg, Virginia 24061.

0022-4715/90/0600-1265$06.00/0

If we denote by f_λ a one-dimensional quadratic map such that

$$x_{n+1} = f_\lambda(x_n) \tag{1}$$

then the period-doubling fixed point is defined as

$$g(x) = \lim_{r \to \infty} \lim_{n \to \infty} (\alpha)^n f^{2^n}_{\lambda_{n+r}}\left(\frac{x}{\alpha^n}\right) = \lim_{n \to \infty} (\alpha)^n f^{2^n}_{\lambda_\infty}\left(\frac{x}{\alpha^n}\right) \tag{2}$$

and satisfies the renormalization equation

$$g(x) = \alpha g\left(g\left(\frac{x}{\alpha}\right)\right) \tag{3}$$

The constant α is calculated numerically to be

$$\alpha = -2.502907875... \tag{4}$$

Sullivan[3] showed that if $f \in C^1$, $f(x) \sim x^2 + f(0)$ for $x \sim 0$ and if the fixed point $g(x)$ exists, then it is universal.

There is another explanation of the constant α. At the superstable parameter λ_n, the critical point 0 is in the orbit. Let d_n be the distance of 0 to the nearest point in the orbit at λ_n. Then d_n/d_{n+1} converges to α.[1]

In this paper we study one-dimensional unimodal maps, but in the chaotic regime, i.e., for parameter value λ greater than the accumulation point of the period-doubling bifurcation. In the next section, we will show how to construct a binary tree which includes all the periodic windows in this chaotic regime. Each periodic window contains a periodic interval and all its doublings. By computing the superstable parameter corresponding to this periodic interval, we get a binary tree composed of numbers on the parameter axis. Viewing this binary tree as a result of bifurcation of some unimodal map, one interesting and important goal is to find the period-doubling fixed point $g(x)$ and the corresponding scaling constant α. In Section 3 we show the renormalization process and numerically compute the period fixed point $g(x)$ and scaling constant α of this special dynamical system for three different maps,

$$h_a(x) = a - x^2 \tag{5}$$

$$h_r(x) = r \sin(\pi x) \tag{6}$$

$$h_\mu(x) = \begin{cases} \dfrac{\mu}{b} x, & 0 \leqslant x \leqslant b \\ \mu, & b \leqslant x \leqslant 1-b \\ \dfrac{\mu}{b}(1-x), & b \leqslant x \leqslant 1 \end{cases} \tag{7}$$

We will use λ to denote the generic parameter hereafter. $\lambda_{\max}$ is defined as the largest parameter such that $h_\lambda(x)$ maps $I \subset \mathbb{R}$ into I. The point x_0 is defined as the left endpoint of $h_{\lambda_{\max}}(x)$. For example, for map (5), $\lambda_{\max} = 2$ and $x_0 = -2$; for maps (6) and (7), $\lambda_{\max} = 1$ and $x_0 = 0$. We shall also discuss the thermodynamics and the scaling function of this system.

As we know, within the chaotic regime there are infinitely many periodic windows. If we were to remove them, only the chaotic part characterized by positive Lyapunov exponent would be left. A natural question to ask is whether there is anything left after this operation, in other words, what is the measure of the chaotic orbits on the parameter axis, or what fraction of the parameter values are chaotic?

Based on the denseness of the periodic intervals, one would be tempted to say that chaos occurs only on a set of measure zero. This is already known to be wrong because of work of Jakobson[5] and the numerical results by Farmer.[6]

Jakobson[5] proved for the two classes of maps (i) $f_\lambda(x) = \lambda f(x)$, where $0 < \lambda \leqslant 4$ and $f_\lambda(x)$ is sufficiently close to $\lambda x(1-x)$ in $C^3([0, 1], [0, 1])$, and (ii) $f_\lambda(x) = \lambda f(x) \pmod 1$, where f is C^3, and $f(1) = f(0) = 0$, f has a unique nondegenerate critical point in $[0, 1]$, that the set of parameter values λ for which f_λ has an invariant measure absolutely continuous with respect to Lebesgue measure has positive (Lebesgue) measure.

Jakobson's work is significant in the sense that it is rigorous, but it could not give further details concerning the magnitude of the measure or any scaling law concerning the behavior of this measure.

In 1985 Farmer[6] computed the chaotic fraction and the "fatness exponent" for two maps,

$$x_{k+1} = f_r(x_k) = r(1 - 2x_k^2) \tag{8}$$

$$x_{k+1} = f_r(x_k) = r \sin(\pi x_k) \tag{9}$$

In both cases, $r \in [0, 1]$.

Defining $h(\varepsilon)$ to be the sum of all the periodic windows whose width is greater than or equal to ε and $\mu(\varepsilon) = 1 - h(\varepsilon)$ [$\mu(\varepsilon)$ is thus a staircase function], he argued that near $\varepsilon = 0$, $\mu(\varepsilon)$ could be approximated by a smooth function. For quadratic maps of intervals, he conjectured that $\mu(\varepsilon)$ asymptotically scales as a power law in the limit as $\varepsilon \to 0$, i.e.,

$$\mu(\varepsilon) \simeq \mu(0) + A\varepsilon^\beta \tag{10}$$

where $\mu(0)$ is the true measure of chaotic parameters, and A is a constant. The "fatness exponent" β is defined as

$$\beta = \lim_{\varepsilon \to 0} \frac{\log[\mu(\varepsilon) - \mu(0)]}{\log \varepsilon} \tag{11}$$

Taking advantage of the symbolic sequences of the periodic orbits, he computed $\mu(\varepsilon)$ by using almost all of the roughly 4000 periodic intervals of size greater than 10^{-8} and found that for map (8), $\mu(0) = 0.89795 \pm 0.00005$ and $\beta = 0.45 \pm 0.04$, while for map (9), $\mu(0) = 0.8929 \pm 0.0001$ and $\beta = 0.45 \pm 0.04$. Based on the results, he conjectured that the value of β is universal for a given order of maximum.

Later Umberger and Farmer[7] computed $\mu(0)$ and β for maps of different orders of maximum.

In this paper we study map (5) on the chaotic regime [1.401155..., 2] as well as Farmer's map (8). We compute the chaotic measure of both maps, and find essential agreement with Farmer's $\mu(0)$ and β for map (8) and find the same β, within error limits, for map (5). We have gone further, to study the scaling of the measure of the periodic intervals on the chaotic regime. The results of $\mu(0)$ and β as well as the new scaling law are presented in Section 4. In Section 5 we present a summary of all the results.

2. NUMERICAL COMPUTATION SCHEME

The details of this section are all known, but we will sketch them for the convenience of the reader.

After introducing the symbolic sequences of a periodic interval, Metropolis *et al.*[8] showed that for a large class of one-dimensional unimodal maps, there exists a universal set of sequences (or patterns) U such that there is a one-to-one correspondence between these sequences and all the periodic intervals. Derrida *et al.*[9] then introduced the law of self-similarity, which says that any composition of sequences in U is also in U and the composition preserves the ordering relation. The sequence corresponding to a periodic interval is defined following ref. 8.

For a given parameter value, if $f^i(0) > 0$, then let $\mu_i = R$; if $f^i(0) < 0$, let $\mu_i = L$; if $f^i(0) = 0$, let $\mu_i = C$ (0 is the critical point). Then the sequence at this parameter will be $\mu_1 \mu_2 \cdots$ if no $\mu_i = C$ and it is $\mu_1 \mu_2 \cdots \mu_k$ if $k+1$ is the smallest integer greater than 1 such that $\mu_{k+1} = C$. If a sequence does correspond to a periodic interval, it is called allowed and the length of the sequence is finite. Not all combinations of R, L, and C are allowed; for example, all the allowed sequences of length greater than 2 must begin with RL. We say a sequence is even if there is an even number of R's in it; otherwise it is odd. The harmonic $H(P)$ of a sequence P is defined to be PRP if P is even and PLP if P is odd. We also define $H^2(P) = H(H(P))$, etc. Similarly, we define the antiharmonic $A(P) = PLP$ if P is even and $A(P) = PRP$ if P is odd and correspondingly $A^i(P)$.

We shall arrange the sequences, or periodic intervals, in a binary tree constructed as follows, according to a theorem of Metropolis *et al.*[8]: From

two sequences $P_1, P_2 \in U$, $P_1 < P_2$ (in the sense that the parameter λ_1 associated with P_1 is less than λ_2 associated with P_2), we find an intermediate sequence as the common beginning part of the sequence $H^\infty(P_1)$ and $A^\infty(P_2)$, denoted by $H^\infty(P_1) \wedge A^\infty(P_2)$. The starting points are the first bifurcation accumulation point λ_∞ [$=3.569945...$ for the logistic map and $=1.40115518909...$ evaluated by Feigenbaum for map (5)] with $P_i = H^\infty(R) = RLR^3LRLRLR^3...$ and the last parameter $\lambda_{\max}$ [$=4$ for the logistic map and $=2$ for map (5)] with $P_f = RL^\infty$ [$= A^\infty(RL^\infty)$]. Applying the rule quoted, we find easily the intermediate sequence $P_1 = RL$, which is the first level of the tree. The second level is $H^\infty(R) \wedge A^\infty(RL) = RLRR$ and $H^\infty(RL) \wedge RL^\infty = RLL$. The rest of the tree is constructed similarly.

For the following analysis we need the superstable parameter value λ_0 for a periodic interval of period p defined by $f_{\lambda_0}^p(c) = c$, where c is the critical point of the map (i.e., the point at which f_λ attains its maximum).

After the binary tree is obtained, the length of each periodic interval can be computed by the following three steps:

1. First find the superstable parameter value λ_0 associated with sequence P. This can be done by using the bisection method as described beow and the following theorem.[4] As defined previously, we say a sequence $P_1 \in U$ is greater than $P_2 \in U$ if the superstable parameter of P_1 is greater than that of P_2. Thus, we have defined a linear ordering on the set of all periodic sequences U by the ordering of the superstable parameters.

Let $P_1 = P^*\mu_1 \cdots$ and $P_2 = P^*\mu_2 \cdots$, where $P^* = P_1 \wedge P_2$. Further, define $R > C > L$.

1. If P^* is even, we say $P_1 < P_2$ if $\mu_1 < \mu_2$.
2. If P^* is odd, we say $P_1 < P_2$ if $\mu_1 > \mu_2$.

The definition extends the ordering relation to all the sequences. Now let λ_i be the parameter value of P_i and let λ_f correspond to P_f. Take $x = c$ and $\bar{\lambda} = (\lambda_1 + \lambda_2)/2$ as the initial condition, where $\lambda_1 = \lambda_i$ and $\lambda_2 = \lambda_f$. Iterate $f_{\bar{\lambda}}$ and thereby construct a sequence P'. Stop when the first character of P' disagrees with the known sequence PC. If $P < P'$, let $\lambda_2 = \bar{\lambda}$ and leave λ_1 unchanged. If $P > P'$, let $\lambda_1 = \bar{\lambda}$ and leave λ_2 unchanged. Then repeat the above process until a stopping criterion which specifies the precision is satisfied.

2. Using λ_0 as obtained above and $x = c$ as the initial conditions, find the left endpoint of the periodic interval by the two-dimensional Newton method, i.e., solve

$$f_\lambda^p(x) = x \tag{12}$$

$$D_x f_\lambda^p(x) = 1 \tag{13}$$

The left endpoint is the solution of the above set. By the construction of the binary tree all the harmonics (i.e., period doublings) of the basic sequence have been excluded. If we want to include their contribution, we need to find the accumulation point of doubling for each sequence, that is, the right endpoint of each periodic interval which can be computed following step 3 below. In this sense a sequence in U represents a periodic window which includes all the harmonics of the interval. On the other hand, a sequence can just represent itself, i.e., a period pth orbit (if the length of P is $p-1$). We shall also need the right endpoint of this "single" interval in this study. It can be obtained by solving Eq. (12) and the equation

$$D_x f_\lambda^p(x) = -1 \tag{14}$$

3. Construct the first k harmonics of P, i.e., $H(P)$, $H^2(P)$,..., $H^k(P)$, where k varies for different P according to their length (i.e., period) and machine character capacity, and compute as in step 1 the corresponding superstable parameter values λ_k. Making use of the fact that

$$\frac{\lambda_k - \lambda_{k-1}}{\lambda_{k+1} - \lambda_k} \to \delta$$

where δ is one of the Feigenbaum exponents,[1] the right endpoint of the periodic window can be approximated by

$$\lambda_R = \lambda_k + \frac{(\lambda_k - \lambda_{k-1})}{\delta} + \frac{(\lambda_k - \lambda_{k-1})}{\delta^2} + \cdots \tag{15}$$

$$\lambda_R = \lambda_k + \frac{\lambda_k - \lambda_{k-1}}{\delta}\left(\frac{1}{1-1/\delta}\right) \tag{16}$$

3. RENORMALIZATION AND THE RESULTS

For a one-dimensional unimodal map $h_\lambda(x)$, if at parameter λ the system $x_{n+1} = h_\lambda(x_n)$ is periodic with period k, there exists a neighborhood of λ for which the system is also periodic with the same period. We call this a periodic interval. As mentioned in the previous section, any periodic interval can be represented by a sequence of letters composed of R, L. Given two different sequences, a third sequence in between (in the sense of the parameter) with minimal length or period can be constructed. From the sequences corresponding to λ_∞ and $\lambda_{\max}$ (= the largest parameter such that h_λ maps $I \subset \mathbb{R}$ into I), we can construct a binary tree of sequences which would exhaust all the periodic "windows" in the chaotic regime. Each sequence can be represented by the superstable parameter value of the

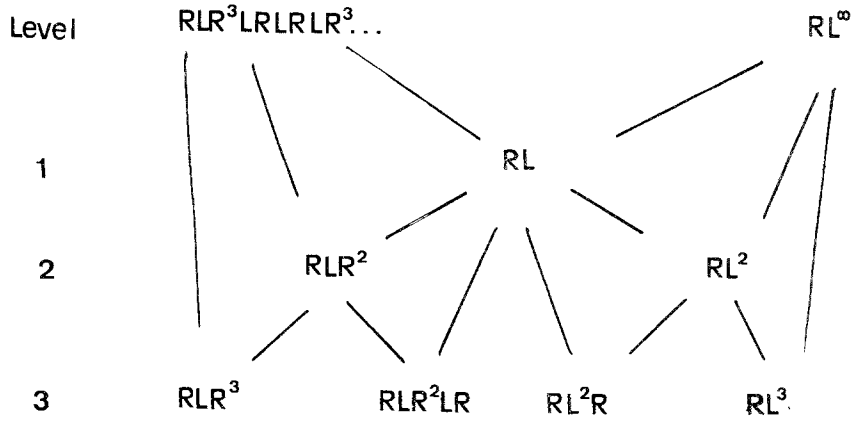

Fig. 1. The first three levels of the binary tree.

periodic interval. Thus, we have a binary tree consisting of parameter values.

Labeling the points in the rth level of the binary tree as in Fig. 2, where the right half are obtained by multiplying the previous level by 2 and the left half are obtained by multiplying previous level by 2, adding 1, and reversing the order, define

$$x_{l+1} = f_r(x_l), \qquad l = 0,..., 2^{r-1} - 1 \tag{17}$$

Letting the limit of f_r as $r \to \infty$ be f_∞, numerical computations show that for $r \geqslant 8$, f_r is a very good approximation to f_∞. Notice that we are making

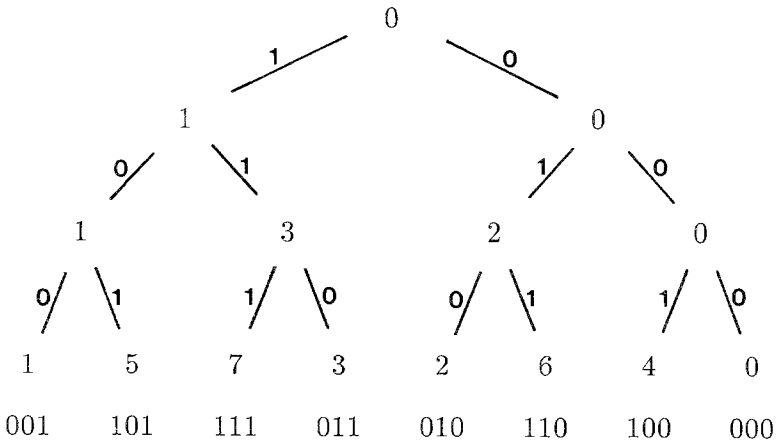

Fig. 2. The binary tree labeled by the subscript of its elements and the binary expansion.

the comparison between the level r of the binary tree and the superstable parameter λ_r of the quadratic map. The rth level of the binary tree can be viewed as the bifurcation orbit of some unimodal map f at parameter r. Similar to the previous renormalization process, we first take the limit $r \to \infty$ (it is equivalent to taking the limit $\lambda_r \to \lambda_\infty$ in the previous case). Then let the number of iteration of f_∞ go to infinity. The nth iterate of f_∞ is defined as $f_\infty^{2^n}$. We show f_∞ and its first and the second iterates for map (5) in Figs. 3–5, respectively.

It is seen from these figures that f_∞ is a unimodal map from $[\lambda_\infty, \lambda_{\max}]$ into itself. It does not have the nice feature of smoothness of a quadratic map. Because of the complexity here, we have to choose a different renormalization approach. An obvious choice is to retain the peak which keeps most characteristics of the corresponding one in the previous iterate. For this reason we use the rightmost peak in each iterate.

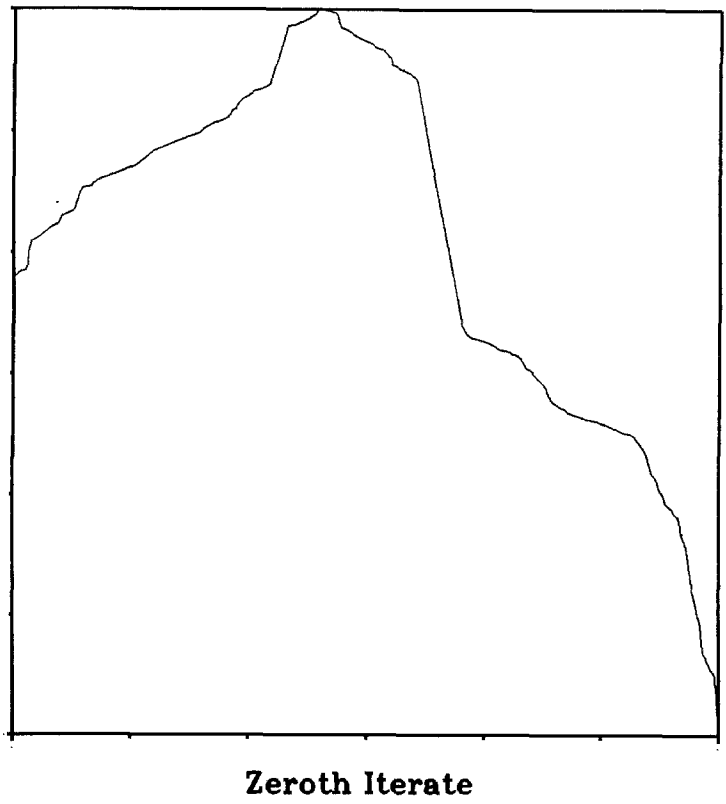

Fig. 3. The graph of f_∞ for map (5).

The numerical computation scheme is as follows: since f_8 is already a good approximation to f_∞, we stop at the level $n=8$, which has 256 points, and make the plot of f_∞ according to Eq. (8). The rightmost peak of the first iterate of f_∞ is given by the rightmost 256 points of the following level, i.e., the ninth level. Likewise, the rightmost peak of the second iterate is obtained from the rightmost 256 point of the tenth level,... . In this way we can compute as many iterates as we like by just concentrating on a branch of the binary tree.

The convergence is very fast here. The fifth iterate, which is shown in Fig. 6 for map (5) (the data points have been extrapolated), is already a good approximation to the fixed point. If we denote the rightmost peak of $f_\infty^{2^n}$ as $f_{\infty,R}^{2^n}$, then $f_{\infty,R}^{2^n}$ is a map from I_n into itself, where $I_n=[\lambda^{(n)}, 2]$. The value of $\lambda^{(n)}$ gets closer to 2 as n increases. By a simple coordinate translation, we can shift the point $(\lambda^{(n)}, \lambda^{(n)})$ to the origin. Let $x_{\max}^n$ be the critical

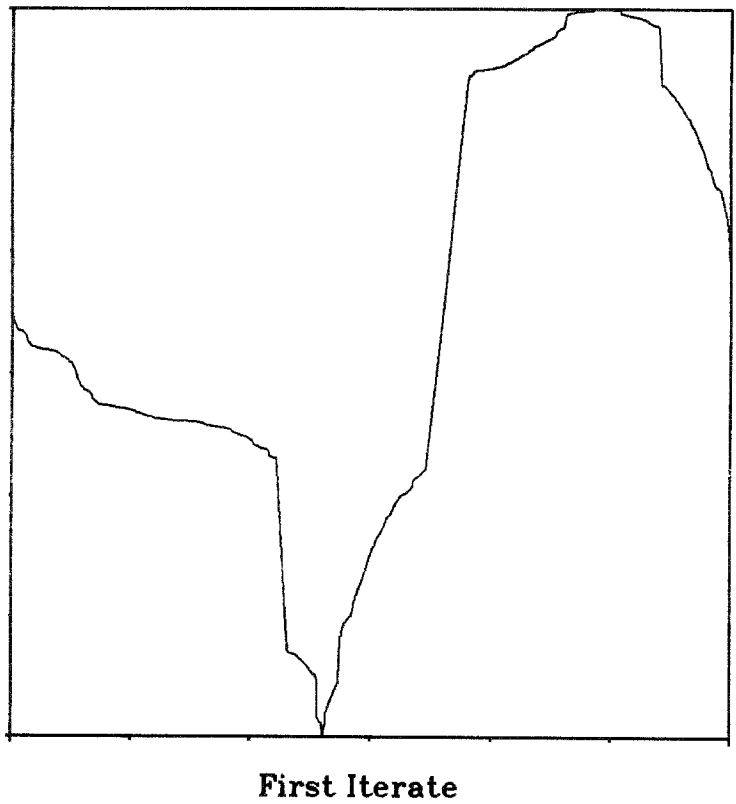

Fig. 4. The first iterate of f_∞, i.e., f_∞^2, for map (5).

point of the $f_{\infty,R}^{2^n}$ and d_n be the distance between $x_{\max}^n$ and the point in the orbit closest to it. The values of $r_n^1 = x_{\max}^n / x_{\max}^{n+1}$, $r_n^2 = f_{\infty,R}^{2^n}(x_{\max}^n)/f_{\infty,R}^{2^{n+1}}(x_{\max}^n)$, and $r_n^3 = d_n/d_{n+1}$ are listed in Table I.

It is seen from Table I that all three ratios converge remarkably well to $\alpha = 4.000000...$, which is exactly the derivative of $h_{\lambda_{\max}}$ at the left endpoint x_0.

We have also computed the limits

$$r_n = \frac{\lambda_{\max} - \lambda^{(n)}}{\lambda_{\max} - \lambda^{(n+1)}} \tag{18}$$

for map (6), and for map (7) in the case of $b = 0.4$ and $b = 0.2$. In all three cases the limits are exactly $h'_{\lambda_{\max}}(x_0)$, namely, $\alpha = \pi$ for map (6), and $\alpha = 2.5$ and $\alpha = 5$ for map (7) with $b = 0.4$ and $b = 0.2$, respectively.

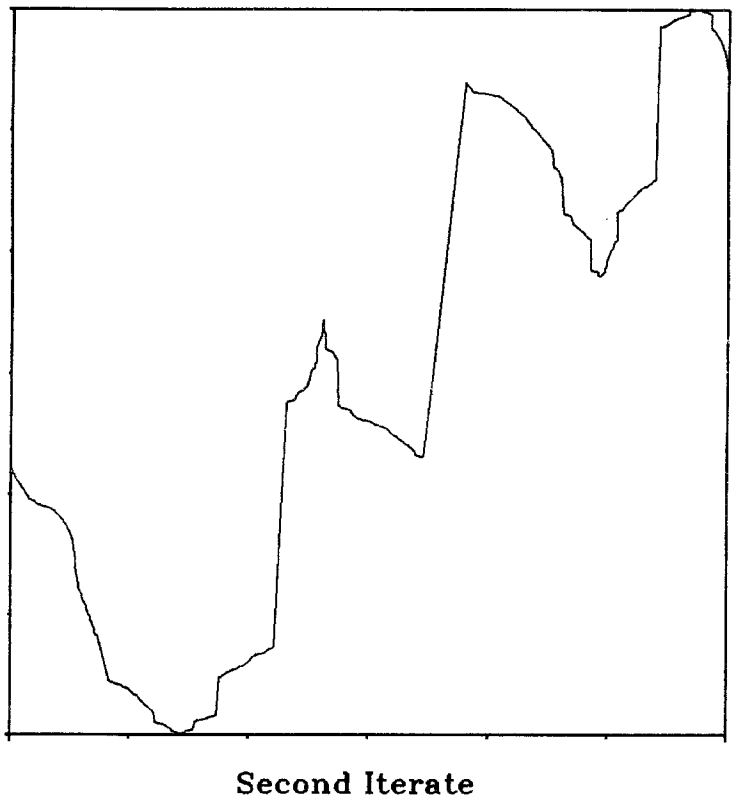

Fig. 5. The second iterate of f_∞, i.e., f_∞^4, for map (5).

If we examine the symbolic sequences of the nth level and $(n+1)$th level of the subtree (i.e., the rightmost 256 sequences of each level of the symbolic binary tree) for large n, we find that the sequences at the $(n+1)$th level are obtained by adding an L to the corresponding ones after the first R in the previous level, i.e., the nth level. When $\lambda^{(n)}$ increases to $\lambda^{(n+1)}$, h_λ increases so that another L is added from the sequence P_1 corresponding to $\lambda^{(n)}$ to form the sequence P_2 corresponding to $\lambda^{(n+1)}$. Examples of P_1 and P_2 are shown in Table II. The sequence corresponding to $\lambda^{(\infty)} = \lambda_{\max}$ is RL^∞. As the number of iterations n increases, the parameter values of the subtree get closer and closer to $\lambda_{\max}$. Therefore the sequences of this subtree get more and more similar to RL^∞. When n is large enough, as mentioned above, only one L is added from the sequence of one level to form the sequence of the next. This process can be seen to depend mainly on the slope of h_λ at the left endpoint, since the majority of the L points are con-

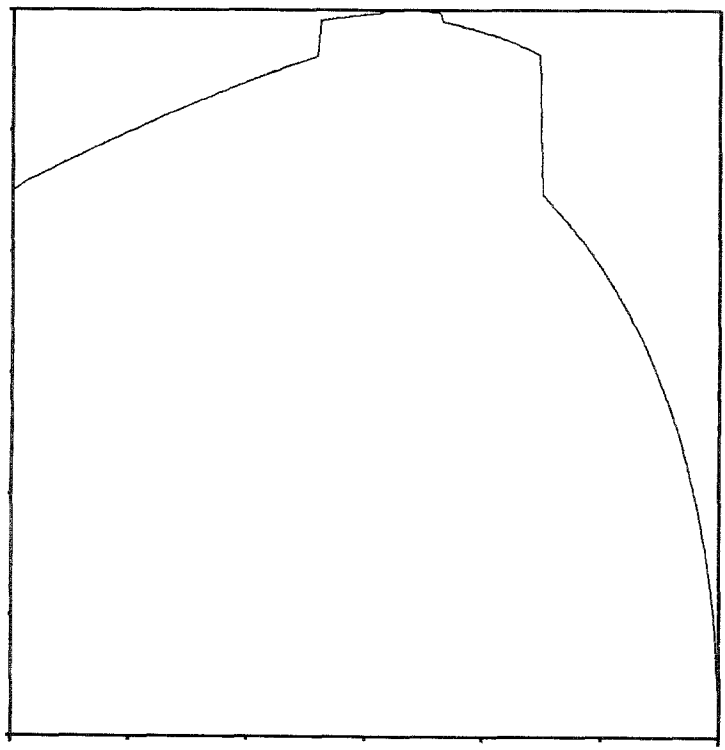

Fig. 6. The rightmost peak of the fifth iterate of f_∞ for map (5).

Table I. Convergence of the Scaling Constant for Map (5)

n	r_n^1	r_n^2	r_n^3
2	3.8077682695888520809	3.5441854060035116563	4.0133945339208604147
3	3.9901636869690091338	3.9483346750336176113	4.0761878217352171634
4	4.0407753272614629430	4.0635553766421511287	4.0329646571576748021
5	3.9935538774560288326	3.9848278793407860822	4.0214917126991557875
6	3.9930896143533401147	3.9863913291596478189	4.0057552362680068389
7	3.9946007211673347841	3.9898760871826001013	4.0015380519756216424
8	3.9962298005893949194	3.9930576799082365042	4.0004095971470468253
9	4.0016510027031824196	4.0029808870688501849	4.0001086905181428164
10	4.0003887390392266206	4.0007009311110452948	4.0000287469118949200
11	4.0000962213534595010	4.0001733204120354695	4.0000075804050993628
12	4.0000240802505799041	4.0000433350555137338	4.0000019935281811335
13	4.0000060422615927655	4.0000108640295424118	4.0000005229893130226
14	4.0000015171038121519	4.0000027253707291892	4.0000001368991833142
15	4.0000003809722066034	4.0000006837955667206	4.0000000357627622612
16	4.0000000956709662525	4.0000001715691122770	4.0000000093251823590
17	4.0000000240249609029	4.0000000430477706629	4.0000000024274185511
18	4.0000000060330601047	4.0000000108008431560	4.0000000006308853790
19	4.0000000015149709363	4.0000000027099376206	4.0000000001637290309
20	4.0000000003804192704	4.0000000006799162198	4.0000000000424341787
21	4.0000000000955239553	4.0000000001705870153	4.0000000000109840174
22	4.0000000000239857733	4.0000000000427987435	4.0000000000028399665
23	4.0000000000060226408	4.0000000000107376852	4.0000000000007333915
24	4.0000000000015122068	4.0000000000026939264	4.0000000000001882541
25	4.0000000000003797132	4.0000000000006758705	4.0000000000000474228
26	4.0000000000000953612	4.0000000000001695243	4.0000000000000201188
27	4.0000000000000239118	4.0000000000000430799	3.9999999999999540143
28	4.0000000000000050594	4.0000000000000083310	4.0000000000002299286
29	4.0000000000000038548	4.0000000000000052617	4.0000000000000000000
30	4.0000000000000038548	4.0000000000000631400	3.9999999999919065126

Table II. Examples of Sequences Related by the Presentation Function

P_1	P_2	P_3
RL^9RL^6	$RL^{10}RL^6$	$RL^9R^2L^6$
RL^9RL^5R	$RL^{10}RL^5R$	$RL^9R^2L^5R$
$RL^9RL^4R^2$	$RL^{10}RL^4R^2$	$RL^9R^2L^4R^2$
RL^9RL^4RL	$RL^{10}RL^4RL$	$RL^9R^2L^4RL$
$RL^9RL^3R^2L$	$RL^{10}RL^3R^2L$	$RL^9R^2L^3R^2L$
$RL^9RL^3R^3$	$RL^{10}RL^3R^3$	$RL^9R^2L^3R^3$
RL^9RL^3RLR	$RL^{10}RL^3RLR$	$RL^9R^2L^3RLR$
$RL^9RL^3RL^2$	$RL^{10}RL^3RL^2$	$RL^9R^2L^3RL^2$

centrated there. Our results and the above argument lead us to conjecture that the scaling constant defined here equals the derivative or slope $h'_{\lambda_{\max}}(x_0)$.

Letting $v = h'_{\lambda_{\max}}(x_0)$, we shall show in the following that

$$\frac{1}{N}\ln(\lambda_{\max} - \lambda^{(n)}) \sim -\ln v \qquad \text{as} \quad n \to \infty \tag{19}$$

where $N > n$ is an integer such that $N = m + n$, and m can be taken as a fixed integer. In the following we shall assume that $n \gg 1$. Letting $\delta_n = \lambda^{(n+1)} - \lambda^{(n)}$, we could approximate the portion of the map close to the left or right endpoint by a linear function as shown in Fig. 7. Letting the first L points corresponding to the sequences of $\lambda^{(n+1)}$ and $\lambda^{(n)}$ be $x_1^{(n+1)}$ and $x_1^{(n)}$, respectively, we have

$$x_1^{(n)} - x_1^{(n+1)} = K\delta_n \tag{20}$$

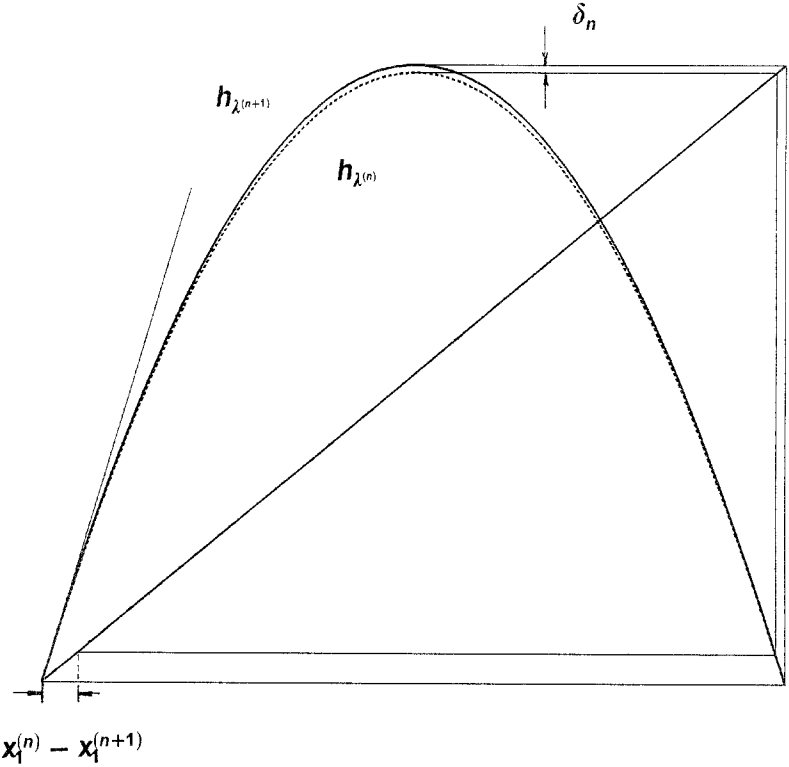

Fig. 7. Illustrative picture for the derivation of Eq. (19).

where K is a constant equal to the absolute value of the slope of the straight line approximating $h_{\lambda^{(n)}} \approx h_{\lambda_{\max}}$ at the right endpoint (Fig. 7).

Suppose that for $x \leqslant \bar{x}$, $h_\lambda(x)$ can be approximated by a linear map with derivative v and there are N of the L's in P_1 and $N+1$ of the L's in P_2 whose values are less than $\bar{x}$. Then for $\varepsilon \ll 1$, $\exists C_1, C_2 \in (\bar{x}-\varepsilon, \bar{x}+\varepsilon)$ such that

$$x_1^{(n)} = C_1 v^{-N} \tag{21}$$

$$x_1^{(n+1)} = C_2 v^{-(N+1)} \tag{22}$$

Combining Eqs. (20)–(22), we have

$$v^{-N} C = \delta_n$$

or

$$\lambda^{(n+1)} - \lambda^{(n)} = C v^{-N} \tag{23}$$

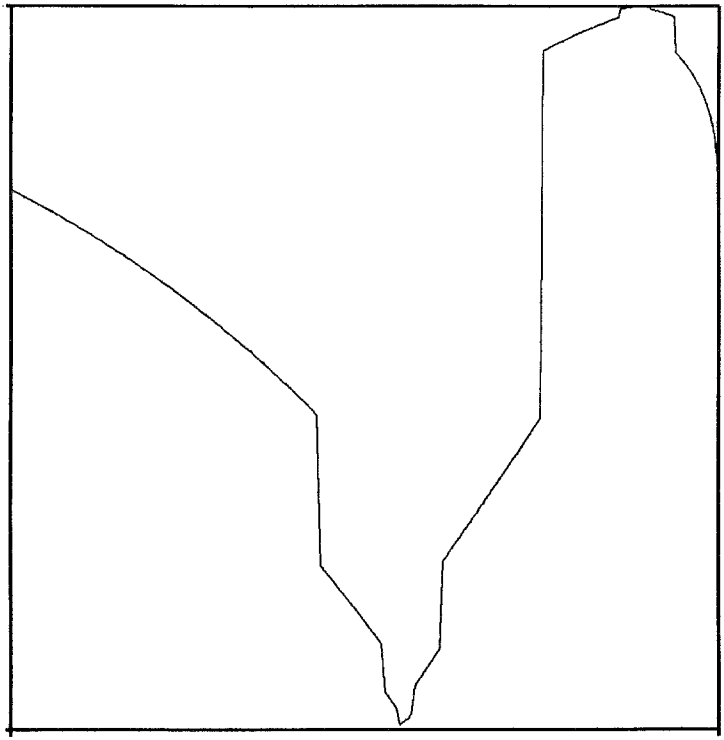

Fig. 8. The first iterate of the period-doubling fixed point g, i.e., $g(g(x))$, for map (5).

where C is a constant. Since

$$\sum_{n}^{\infty} (\lambda^{(k+1)} - \lambda^{(k)}) = \lambda^{(\infty)} - \lambda^{(n)} = Cv^{-N}\left(1 + \frac{1}{v} + \frac{1}{v^2} + \cdots\right) = C'v^{-N}$$

where C' is a constant, by taking the logarithm of above equation, we have

$$\frac{1}{N}\ln(\lambda^{\infty} - \lambda^{(n)}) = \frac{1}{N}\ln(\lambda_{\max} - \lambda^{(n)}) = \frac{C'}{N} - \ln v \sim -\ln v, \qquad n \to \infty$$

which is Eq. (19). It will further give the convergence of (18) as the level $n \to \infty$.

A plot of $g(g(x))$ for map (5) is shown in Fig. 8. Now $\lambda_{\max}$ is the fixed point of the renormalization operation. Thus, in order that the period-doubling fixed point $g(x)$ satisfy an equation like Eq. (3), we will have to

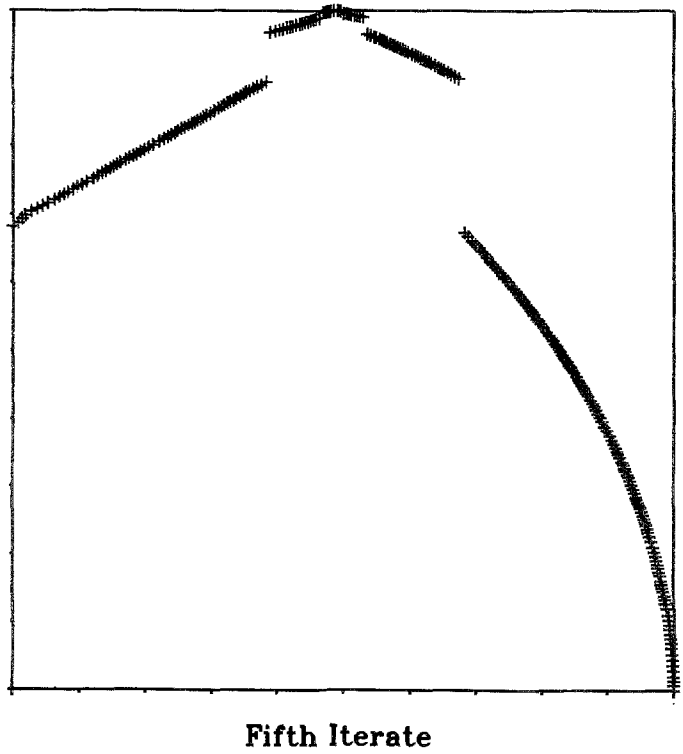

Fig. 9. The period-doubling fixed point for map (6).

make a coordinate transformation so that $\lambda_{\max}$ is the origin. Then $g(x)$ satisfies

$$\alpha g\left(g\left(\frac{x}{\alpha}\right)\right) = g(x), \qquad x \in [-1, 0] \tag{24}$$

where $\alpha = h'_{\lambda_{\max}}(x_0)$. The period-doubling fixed points for maps (6) and (7) with $b = 0.4$ are shown in Figs. 9 and 10, respectively. It is seen that $g(x)$ depends on the details of the unimodal maps while the scaling constant equals exactly the derivative of $h_{\lambda_{\max}}$ at the left endpoint.

Starting from the point $x = 0$ and defining

$$x_r = g^r(0) \qquad \text{for} \quad r \geqslant 1 \tag{25}$$

we get a set of points which are the trajectory of $g(x)$ under the initial condition $x = 0$. These points can be described by the intervals covering them. The crudest approximation is to cover it by $[x_1, x_0]$, which is called the

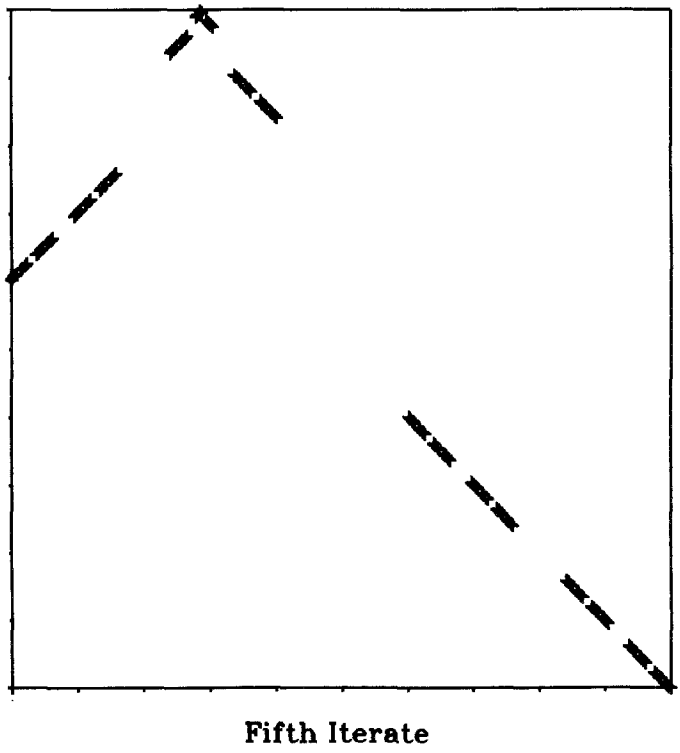

Fig. 10. The period-doubling fixed point for map (7) with $b = 0.4$.

first level. A better approximation would be to cover it by two intervals $[x_1, x_3]$ and $[x_2, x_0]$ as the second level. We can get better and better approximations when the level n increases. Since

$$x_{2r} = g^{2r}(0) = (g^2)^r(0) = \alpha^{-1} g^r(0) = \alpha^{-1} x_r$$

and

$$x_{2r+1} = g^{2r+1}(0) = g(g^{2r}(0)) = g(\alpha^{-1} x_r)$$

we can define

$$x_{2r}^{(n+1)} = F_0(x_r^{(n)}) \tag{26}$$

$$x_{2r+1}^{(n+1)} = F_1(x_r^{(n)}) \tag{27}$$

where $F_0 = \alpha^{-1}$ and $F_1 = g \circ \alpha^{-1}$.

The map E composed of F_0^{-1} and F_1^{-1} is the presentation function introduced previously by Feigenbaum.[10,11] As seen in Fig. 11 [map (5)],

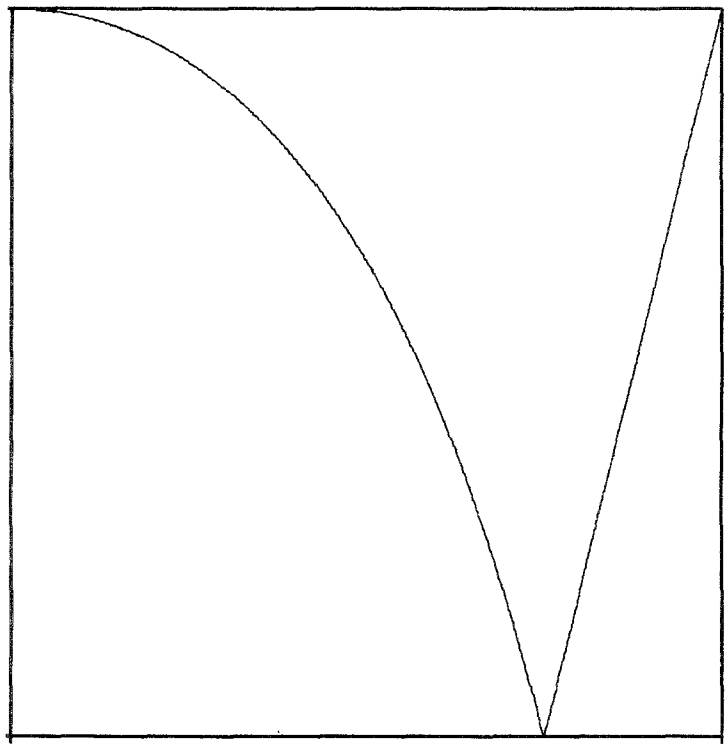

Fig. 11. The presentation function E for map (5).

unlike the situation in the renormalization for the quadratic maps, here F_0^{-1} instead of F_1^{-1} is a straight line with slope α. This results from the different renormalization procedure we use here. As pointed out by Feigenbaum,[11] the forward dynamics generated by the period-doubling fixed point g is the same as the backward dynamics generated by the presentation function E.

In Table II, some sequences of level seven and eight are given. F_0 is obtained by plotting the superstable parameters of P_2's against those of P_1's. From the results of the previous section [Eq. (19)], we know that $\alpha = \nu = h'_{\lambda_{\max}}(x_0)$. Accordingly, F_1 is obtained by plotting the superstable parameters of P_3's against those of P_1's. As shown in the table, P_3 can be derived from the corresponding P_1 by adding an R after the second R in P_1.

When we are doing the renormalization operation, we keep only the rightmost peak, i.e., we focus only on the rightmost subtree of the binary tree. We will label this subtree by the binary expansion as seen in Fig. 2. The scaling function of a point in the orbit is defined as[11]

$$\sigma(\varepsilon_m \cdots \varepsilon_0) = \frac{x_{0\varepsilon_m \cdots \varepsilon_0} - x_{1\varepsilon_m \cdots \varepsilon_0}}{x_{\varepsilon_m \varepsilon_{m-1} \cdots \varepsilon_0} - x_{\bar{\varepsilon}_m \varepsilon_{m-1} \cdots \varepsilon_0}} \tag{28}$$

The result of the scaling function of the subtree is shown in Fig. 12. As seen in the figure, the scaling function is almost a constant ($=0.33$). The scaling

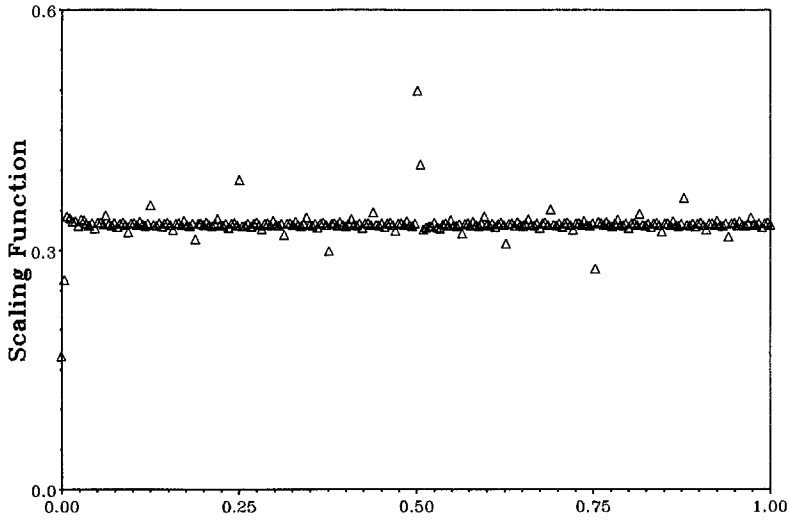

Fig. 12. The scaling function σ for map (5) plotted against the normalized subscript of the points in the orbit.

function for map (7) is a constant, 0.28576 and 0.166667 for $b=0.4$ and $b=0.2$, respectively. The scaling function for map (6) is shown in Fig. 13, and can be described by a piecewise constant function.

Feigenbaum[11] proved that for quadratic maps if F_0 is piecewise linear (F_1 is linear), then the scaling function is piecewise constant. Here F_0 is linear, but F_1 is not piecewise linear. The numerical results still agree with the proof.

The scaling function compares the size of two adjacent points in the orbit of a certain level with that of two corresponding points in the orbit of the previous level. The universal constant α is the scaling factor governing the distance of any point in the orbit relative to the origin after one iteration. Both of them indicate that there exists a constant scaling in this system.

Because of the similarity between the sums used to compute the Hausdorff dimension and the partition sum in thermodynamics, the term "partition sum" will be referred to,[12]

$$Z_N(\beta)=\sum_{i=1}^{N} l_i^{\beta} \tag{29}$$

where $N=2^{n-1}$ and l_i is the length of a pair of adjacent points in the nth level of the binary tree.

Suppose, for $\beta=D$,

$$\lim_{N\to\infty} Z_N(D)=O(1) \tag{30}$$

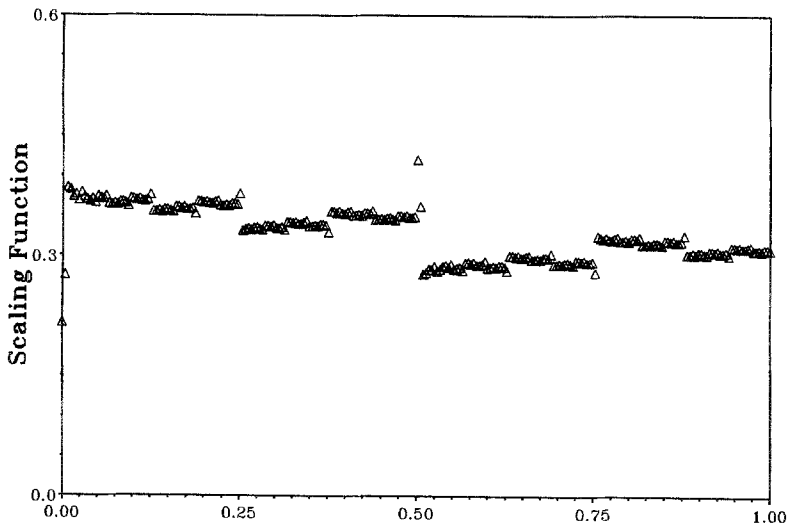

Fig. 13. The scaling function σ for map (6) plotted against the normalized subscript of the points in the orbit.

Then D is an upper bound of the Hausdorff dimension D_H. D is the Hausdorff dimension if the covering is optimal.

In the present situation $\ln N$ corresponds to the thermodynamic degrees of freedom, and so the quantity which has a finite limit is

$$q_N(\beta) = \frac{1}{\ln N} \ln Z_N(\beta) \tag{31}$$

When $\beta = D$, Eq. (30) becomes

$$\lim_{N \to \infty} q_N(D) = 0 \tag{32}$$

We have computed $q_N(\beta)$ for $n = 8,..., 13$ where $N = 2^{n-1}$. The results are shown in Fig. 14. One conclusion we can draw from the figure is that there is no phase transition occurring in the system. It is seen from the

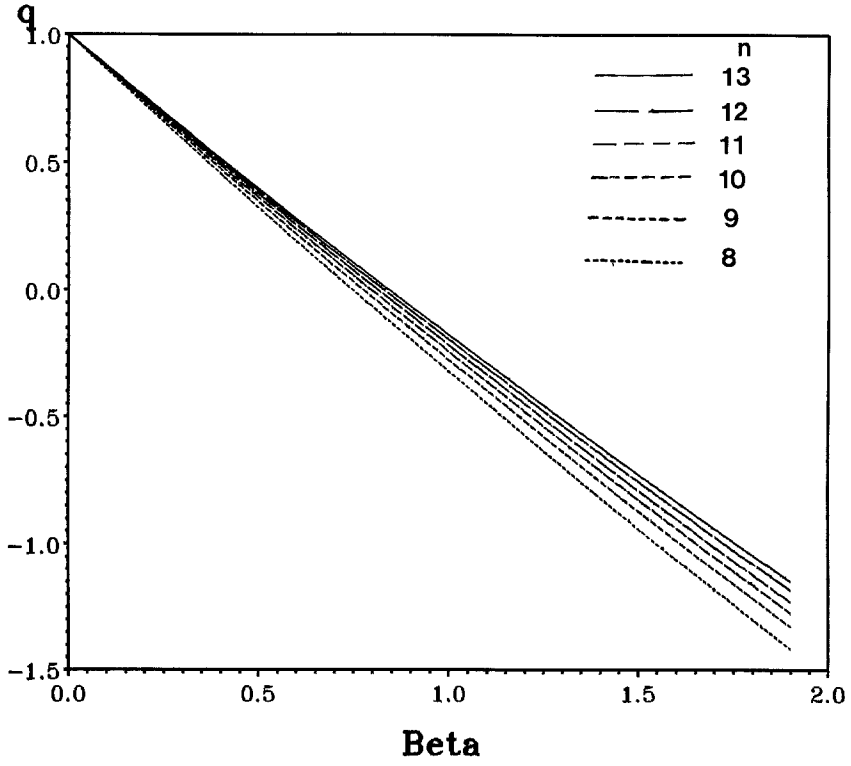

Fig. 14. The "partition function" [map (5)] plotted against the "temperature" for $n = 8,..., 13$.

figure that as n increases, $q_N(\beta)$ also increases. Since there is no gap in the presentation function, it is certain that the Hausdorff dimension of this system is 1.

4. THE SCALING OF MEASURES OF PERIODIC INTERVALS

From Section 2 we know that the binary tree is infinite, with the number of periodic intervals doubling as the level increases from n to $n+1$. How will the size or length of the nth level of the binary tree behave as n goes to infinity? [The numerical results in this section are obtained for map (5) unless otherwise specified.]

One easy experiment is to consider some special periodic intervals such as RL^n which is numerically found to be the smallest interval of period $n+2$. (Here "small" refers to the length.) Also, RL^n is the rightmost sequence of level n in the tree. Now, following the procedures in the last section, the length of the single periodic interval RL^n is computed. In Fig. 15 the ratio of the length of RL^{n+1} to the length of RL^n is plotted, with the variable being the period of RL^n. As the period increases, the ratio goes to a number, 0.0625, which is much less than 1. For the sequences like RLR^n similar calculations are performed. The resulting curve is shown in Fig. 16. Notice that the ratio converges to a different number, 0.3549, and it is also less than 1. For sequences like $RLRRR(LR)^n$, behavior similar to Fig. 16 is observed, the ratio being approximately 0.33.

For the periodic interval represented by RL^n, let the left endpoint be $\lambda_L^{(n)}$ and the right endpoint be $\lambda_R^{(n)}$. The critical point 0 is no longer in the periodic orbit of $\lambda_L^{(n)}$ or $\lambda_R^{(n)}$. Instead, x_L^* or x_R^* in the neighborhood of 0 is in the orbit, respectively, for $\lambda_L^{(n)}$ and $\lambda_R^{(n)}$. Starting from x_L^* or x_R^*, we can construct also a symbolic sequence.[4] Letting $x_L^{(0)}$, $x_R^{(0)}$ be the first point and $x_L^{(1)}$, $x_R^{(1)}$ be the second point in the construction, respectively, we have

$$x_L^{(1)} = \lambda_L^{(n)} - (x_L^{(0)})^2$$
$$x_R^{(1)} = \lambda_R^{(n)} - (x_R^{(0)})^2$$

Therefore,

$$\lambda_R^{(n)} - \lambda_L^{(n)} = x_R^{(1)} - x_L^{(1)} + (x_R^{(0)})^2 - (x_L^{(0)})^2$$

$x_R^{(1)} - x_L^{(1)}$ is negligible compared to the second term in the above expression; hence

$$\lambda_R^{(n)} - \lambda_L^{(n)} \approx (x_R^{(0)})^2 - (x_L^{(0)})^2$$

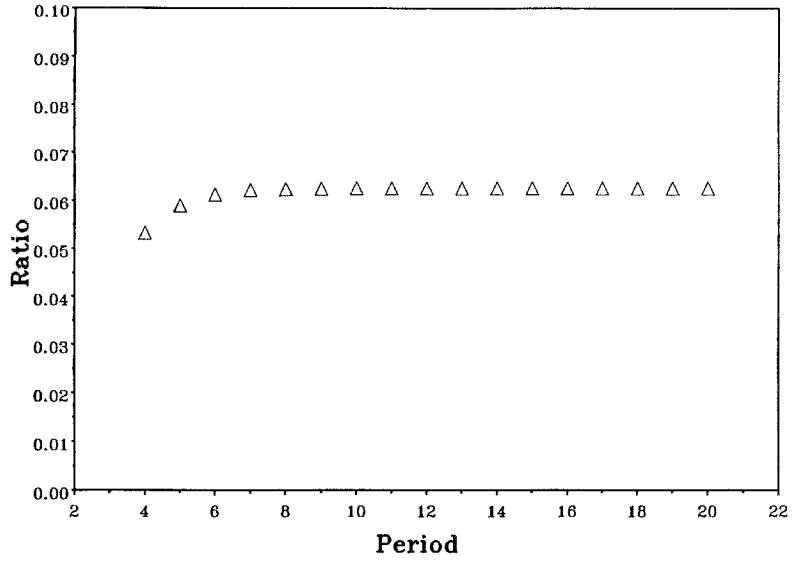

(a)

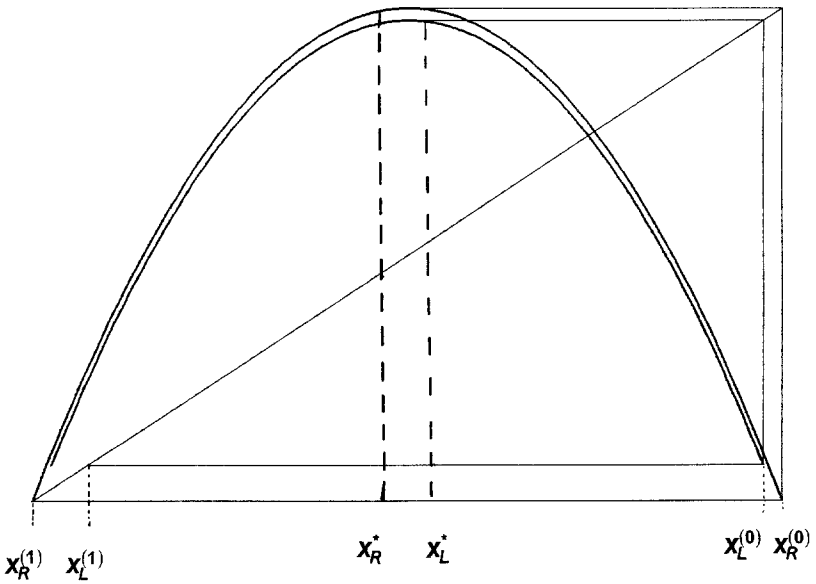

(b)

Fig. 15. (A) The ratio of the length of the periodic interval RL^{n+1} to that of RL^n, plotted against the period of RL^n. (B) The illustrative graph for deriving Eq. (34).

Similar to the argument in deriving Eq. (20), $\exists C_1, C_2$ such that

$$x_R^{(1)} = C_1 v^{-N}$$
$$x_L^{(1)} = C_2 v^{-N}$$

where C_1 and C_2 are constants, $n = N + m$, where m is fixed and v is the left-hand derivative of $h_{\lambda_{\max}}$. It is easy to see that $\exists C_1'$ and C_2' such that

$$x_R^{(0)} = 2 - C_1' v^{-N}$$
$$x_L^{(0)} = 2 - C_2' v^{-N}$$

We have

$$\lambda_R^{(n)} - \lambda_L^{(n)} \approx 2(C_2' - C_1') v^{-N} + [(C_2')^2 - (C_1')^2] v^{-2N} \approx [(C_2')^2 - (C_1')^2] v^{-2N}$$

Therefore,

$$\frac{1}{2N} \ln(\lambda_R^{(n)} - \lambda_L^{(n)}) \sim -\ln v \qquad n \to \infty \tag{33}$$

which gives for map (5),

$$\frac{m(RL^{n+1})}{m(RL^n)} \sim v^{-2} = 0.0625 \tag{34}$$

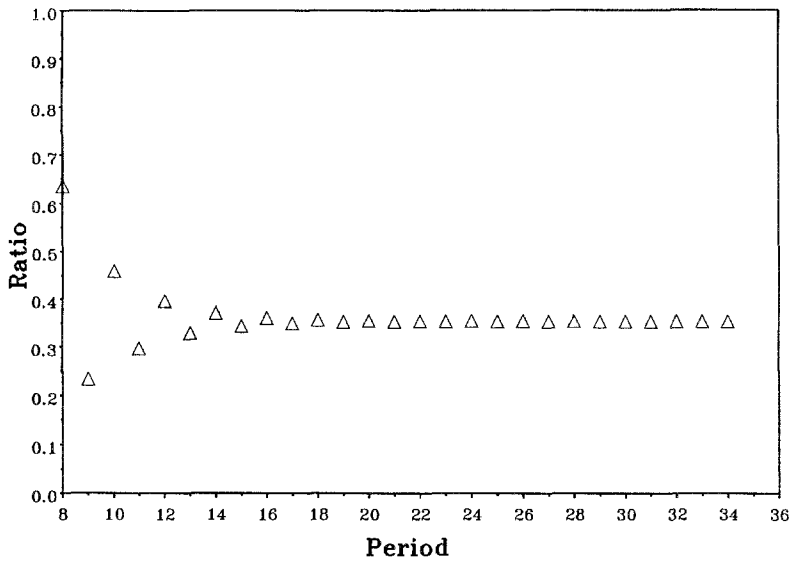

Fig. 16. The ratio of the length of the periodic interval RLR^{n-1} to that of RLR^n, plotted against the period of RLR^n.

The analysis for the other sequences such as RLR^n is more complicated and will not be given here. The above computation is done for only some special sequences. The result still gives us evidence that the sum of the length of level n will go to zero as n goes to infinity.

Another interesting experiment is to make use of the law of internal similarity[9] and examine the relationship between the scaling constant and the length of a "single" periodic interval. The composition $*$ of two allowed sequences P and $Q = \mu_1 \mu_2 \cdots \mu_k$ ($\mu_i = R, L$) is defined as

$$P * Q = P\tau_1 P\tau_2 \cdots P\tau_k P$$

where $\tau_i = \mu_i$ if P is even and $\tau_i = \overline{\mu_i}$ if P is odd ($\bar{R} = L$ and vice versa). By the law of internal similarity, for any allowed sequences P and Q, $P * Q$ is also allowed. Therefore, the sequences P, $P * Q$, $(P * Q) * Q = P * Q^{*2}$, $P * Q^{*3}$,... are also allowed. Let λ_n be the superstable parameter values corresponding to $P * Q^{*n}$, and define $\delta_n(Q)$ as

$$\delta_n(Q) = \frac{\lambda_n - \lambda_{n-1}}{\lambda_{n+1} - \lambda_n} \tag{35}$$

and δ'_n as

$$\delta'_n(Q) = \frac{m(P * Q^{*n})}{m(P * Q^{*}(n+1))} \tag{36}$$

where $m(P * Q^{*n})$ refers to the measure of the single period interval represented by $P * Q^{*n}$.

Let P be any allowed sequence and $Q = R$. The past numerical results[1] show that the sequences $\delta_n(R)$ and $\delta'_n(R)$ converge to $\delta = 4.6692...$, where δ is the Feigenbaum exponent and is independent of P. Since R is the only period-2 sequence, there is only one doubling sequence. In other words, the bifurcation of a sequence is generated only by its composition with R infinitely many times.

Now consider the only period-3 sequence RL, and let $Q = RL$. By constructing $P * Q^{*n} = P * (RL)^{*n}$, we get a sequence of tripling sequences. The corresponding $\delta_n(RL)$ and $\delta'_n(RL)$ converge to another scaling constant $\delta_{RL} = 55.247$[9] which is independent of P. There are two period-4 periodic intervals. One is RLR, which is just $R * R$, so that the scaling constant of the sequence with $Q = RLR$ is the square of the scaling constant of $Q = R$. Another is RLL, the scaling constant of which is 981.595. We checked that $\delta_n(Q)$ and $\delta'_n(Q)$ have the same limit in both cases, independent of P.

This can be understood by Feigenbaum's result,[1]

$$\lambda_n(u) - \lambda(0) \sim a(u)\, \delta^{-n}$$

where u is the stability, i.e., $u = D_x f_\lambda^p(x)$. Then the endpoints Λ_n^R and Λ_n^L obey $\Lambda_n^R = \lambda_n(-1)$ and $\Lambda_n^L = \lambda_n(1)$. Thus,

$$\Lambda_n^R - \Lambda_n^L \sim [a(-1) - a(1)]\, \delta^{-n}$$

Hence we see that $\delta_n'(Q) \to \delta_Q$.

Therefore, for any sequence P, $P * Q$, $P * Q^{*2}$,..., where P and Q are arbitrary allowed sequences, $\delta_n(Q)$ and $\delta_n'(Q)$ converge to the same limit and they are independent of P. Hence a sequence Q can be characterized by the scaling constant of the sequence and by its length.

In Table III the length of some sequences and the corresponding scaling constants are listed. It is seen from the table that the "shorter" the length, the larger the scaling constant, which indicates that for a fixed sequence P the length of $P * Q$ depends on the length of Q as Q varies. If the length of Q is larger, so is the length of $P * Q$. The product of the length and the scaling constant for the sequences listed in the table is very close to 1. While all the sequences with period less than 7 are included, only some of the sequences of period 8–10 have been chosen arbitrarily. Due to the limitation of the computer in handling characters, only the first three elements of the sequence $\{\delta_n(Q)\}$ were computed, so these results are to be considered only indicative.

Let $\delta_n(Q) = m(P * Q^{*n})/m(P * Q^{*(n+1)})$ and $\delta_n(Q) \to \delta_Q$ as $n \to \infty$. The numerical results can be summarized as

$$\delta_Q m(Q) \sim 1 \tag{37}$$

or

$$\frac{m(P * Q^{*n})\, m(Q)}{m(P * Q^{*(n+1)})} \sim 1 \qquad \text{as} \quad n \to \infty \tag{38}$$

As the period of the sequence Q increases, Eq. (35) becomes more accurate and also the convergence $\delta_n(Q) \to \delta_Q$ is faster.

Let S_n be the sum of the nth-level periodic measure and T_n be its partial sum up to level n, i.e.,

$$T_n = \sum_{k=1}^{n} S_k$$

In Figs. 17 and 18 the partial sum T_n vs. level n is plotted for maps (5) and (8), respectively. For map (5) the computation is done up to level 13 with a total of 8191 periodic windows. The result is $T_\infty = 0.0605 \pm 0.0002$. For map (8) it is done to level 12 with 4095 periodic windows, with $T_\infty = 0.0165 \pm 0.0001$. As seen in these figures the partial sum in both cases converges as the level increases.

Table III. The Length, Scaling Constants, and Their Product for Some Sequences

Period	Pattern Q	Length $m(Q)$	δ_Q	$\delta_Q m(Q)$
2	*R*	0.5000E00	0.4669E + 1	2.335
3	*RL*	0.1853E − 1	0.5525E + 2	1.024
4	*RLR*	0.1181E00	0.2180E + 2	2.575
	RLL	0.9870E − 3	0.9816E + 3	0.9688
5	*RLRR*	0.4039E − 2	0.2555E + 3	1.032
	RLLR	0.7781E − 3	0.1287E + 4	1.001
	RLLL	0.5813E − 4	0.1693E + 5	0.9841
6	*RLRRR*	0.5041E − 2	0.2184E + 3	1.101
	RLLRL	0.8693E − 2	0.2184E + 3	1.899
	RLLRR	0.1176E − 3	0.8508E + 4	1.001
	RLLLR	0.3560E − 4	0.2802E + 5	0.9975
	RLLLL	0.3562E − 5	0.2791E + 6	0.9941
7	*RLRRRR*	0.6946E − 3	0.1447E + 4	1.005
	RLRRLR	0.4472E − 3	0.2254E + 4	1.008
	RLLRLR	0.9848E − 4	0.1017E + 5	1.002
	RLLRRR	0.4380E − 4	0.2284E + 5	1.000
	RLLRRL	0.2839E − 4	0.353 E + 5	1.002
	RLLLRL	0.1569E − 4	0.636 E + 5	0.9979
	RLLLRR	0.5979E − 5	0.1672E + 6	0.9997
	RLLLLR	0.2050E − 5	0.4874E + 6	0.9992
	RLLLLL	0.2212E − 6	0.451 E + 7	0.9976
8	*RLRRLRR*	0.1731E − 3	0.583 E + 4	1.009
	RLLRLRR	0.5087E − 4	0.1968E + 5	1.001
	RLLRLRL	0.3801E − 4	0.265 E + 5	1.007
	RLLRRRL	0.2676E − 4	0.3729E + 5	0.9979
	RLLRRRR	0.9824E − 5	0.1018E + 6	1.000
	RLLLLRR	0.3526E − 6	0.2835E + 7	0.9996
9	*RLRRRRRR*	0.1039E − 3	0.960 E + 3	0.9974
	RLRRRRLR	0.1266E − 3	0.792 E + 3	1.002
	RLLRRRLR	0.4016E − 5	0.2491E + 6	1.000
	RLLLRLLR	0.1518E − 5	0.6584E + 6	0.9995
	RLLLRRLL	0.3486E − 6	0.287 E + 7	1.000
10	*RLRRRLRLR*	0.9235E − 3	0.111 E + 4	1.025
	RLRRRRRLR	0.2242E − 3	0.4523E + 4	1.024
	RLLRRRRRL	0.1341E − 5	0.7454E + 6	0.9996
	RLLLRRLRL	0.9955E − 7	0.1005E + 8	1.000

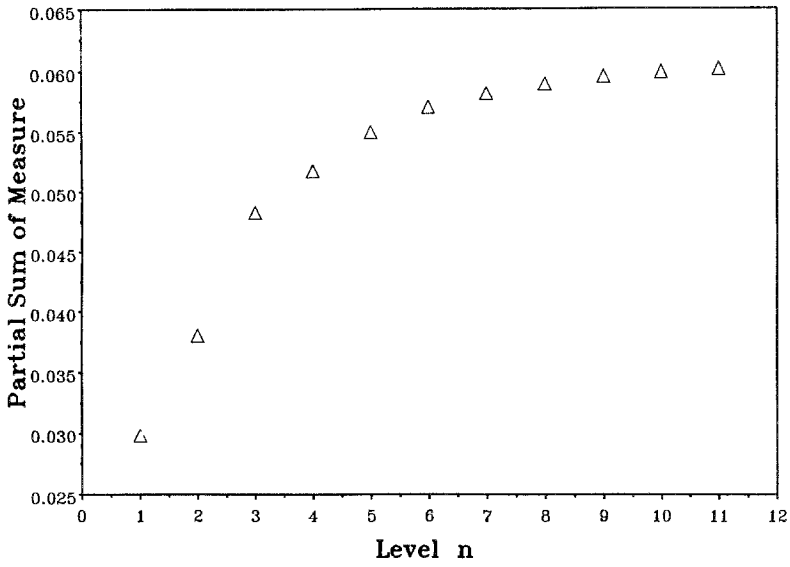

Fig. 17. The partial sum T_n of the length of the periodic windows in the first n levels of the binary tree for map (5) plotted against the level of the binary tree n.

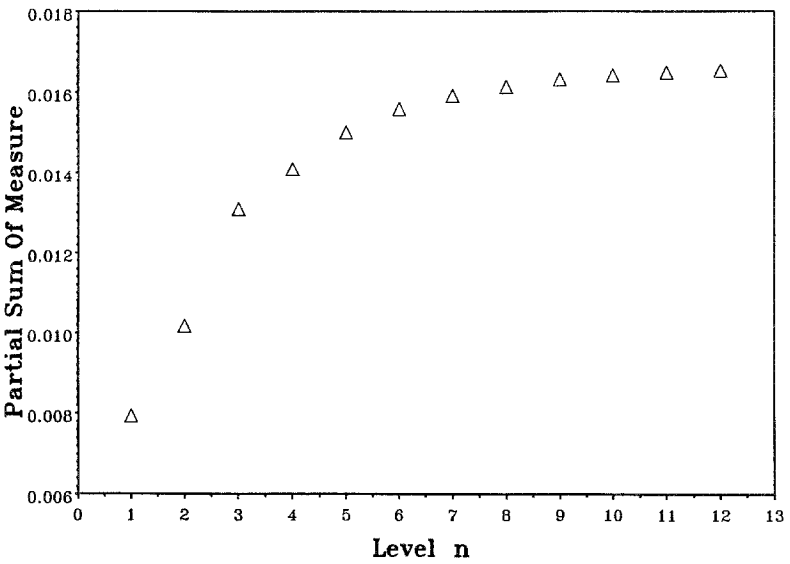

Fig. 18. The partial sum T_n of the length of the periodic windows in the first n levels of the binary tree for map (8) plotted against n.

It is conjectured that T_n converges as $n \to \infty$ with the same asymptotic behavior for maps of the same order of maximum. This is supported by Fig. 21 which shows the normalized partial sum vs. n for map (5) (the data points represented by $\triangle$) and for map (8) (the data points represented by $+$).

For map (5), $a_\infty = 1.401155$ and $a_{\max} = 2$. The percentage of the chaotic orbits in the chaotic regime is

$$\mu(0) = \frac{(a_{\max} - a_\infty) - T_\infty}{a_{\max} - a_\infty}$$

$\mu(0) = 0.8990 \pm 0.0003$.

For map (8), $r_\infty = 0.837005$ and $r_{\max} = 1$. The percentage of the chaotic orbits in the chaotic regime is

$$\mu(0) = \frac{(r_{\max} - r_\infty) - T_\infty}{r_{\max} - r_\infty}$$

and $\mu(0) = 0.8985 \pm 0.0007$.

Farmer included all the windows with length greater than 10^{-8} for map (8). Twelve levels have been computed here. It is certain that some periodic windows with length greater than 10^{-8} have not been included. Our results of $\mu(0)$ could be a little overestimated. In any event, our result is consistent with Farmer's result, $\mu(0) = 0.89795 \pm 0.00005$, within stated error.

Next, we want to determine the critical exponent β defined by Eq. (11). Because we used the tree construction, we really know $\mu_n(\varepsilon)$, i.e., only periodic windows that appear in the first n levels of the binary tree are taken into account. Obviously,

$$\mu_n(\varepsilon) \geqslant \mu(\varepsilon)$$

and

$$\mu_n(\varepsilon) \to \mu(\varepsilon) \qquad \text{as} \quad n \to \infty$$

Figure 19 shows $\Delta\mu_n(\varepsilon) = \mu_n(\varepsilon) - \mu(0)$ for map (5) with $n = 10$ and $n = 11$. Similarly, Fig. 20 shows $\Delta\mu_{10}(\varepsilon)$ and $\Delta\mu_{12}(\varepsilon)$ for map (8). Because of the logarithmic scale, the graphs are essentially straight lines with slope β. The reason for the deviation from the straight line for $\varepsilon \leqslant 2^{-17}$ is that $n = 12$ is not large enough to include all the intervals with length bigger than or equal to ε and some of these intervals appear on the lower levels of the binary tree. As n increases, this deviation gets smaller, suggesting that it disappears in the limit of $n \to \infty$ as Farmer conjectured. The values of β

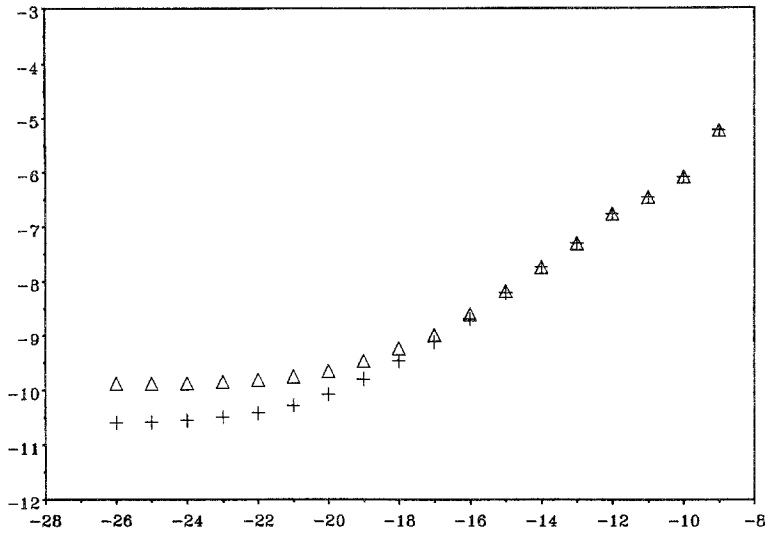

Fig. 19. Plot of $\log_2 \Delta\mu_n(\varepsilon)$ against the resolution $\log_2 \varepsilon$ for map (5), for (+) $n = 11$, (△) $n = 10$.

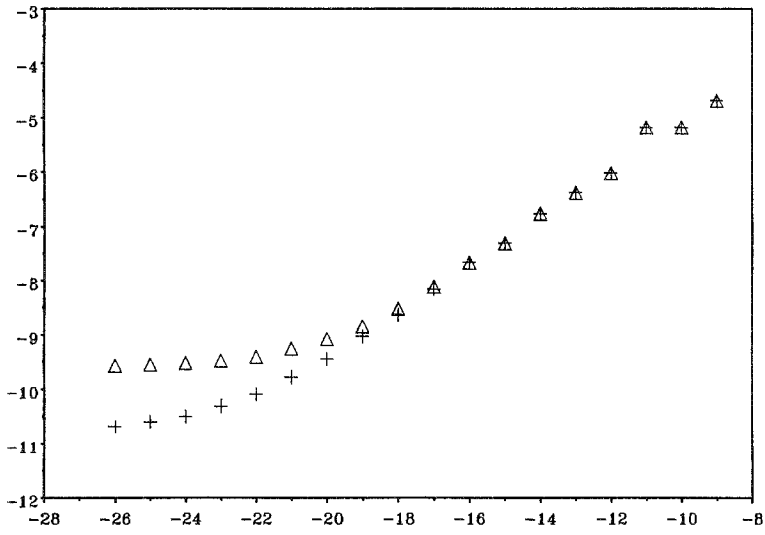

Fig. 20. Plot of $\log_2 \Delta\mu_n(\varepsilon)$ against $\log_2 \varepsilon$ for map (8), for (+) $n = 12$, (△) $n = 10$.

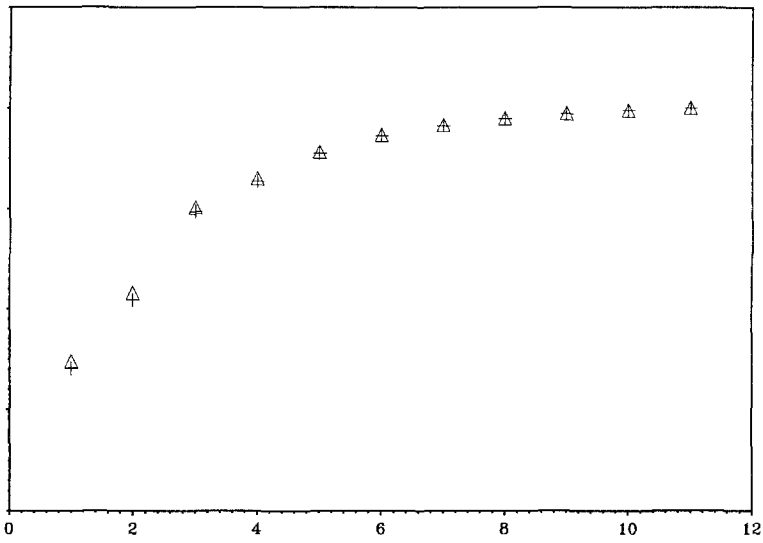

Fig. 21. The normalized partial sum vs. n for map (5) ($\triangle$) and map (8) ($+$)

for both maps fall roughly into the range of Farmer's results, i.e., $\beta = 0.45 \pm 0.04$, but still it is difficult to conclude from the numerical data that β is the same for both maps as conjectured by Farmer.[6]

All the computations have been performed in 16-byte arithmetic (128 bits).

5. SUMMARY AND DISCUSSION

We have thoroughly investigated the dynamical system (a one-dimensional unimodal map) derived from the symbolic binary tree of one-dimensional unimodal maps. The corresponding period-doubling fixed point $g(x)$ and the scaling constant α are found after applying a renormalization operation. The period-doubling fixed point is found to depend on the details of the original unimodal map, while the scaling constant equals the left endpoint derivative of the original map at the largest parameter value. This approach of analysis can be applied to any kind of binary tree. In this study we use the superstable parameter value of the periodic interval in the tree, i.e., the parameter value such that $u = 0$. We expect to get the same results by using parameter values such that the stability $u = a$, where $|a| \leqslant 1$ instead.

The presentation function and the scaling function are also computed. Because of the special properties of this system, they are different from the

results of one-dimensional quadratic maps. The thermodynamics of the system is discussed. It is found that there is no phase transition.

As we have seen, periodic windows in the chaotic regime exhibit a remarkably rich structure. In order to study this structure, we constructed approximately 8000 periodic windows, organized on a complete binary tree. Then we used this construction to calculate the percentage of chaotic orbits in the chaotic regime. Our results confirm the results of Farmer. We also found that the product of the scaling constant of the sequence Q and the length of the corresponding interval $m(Q)$ approximately equals 1.

ACKNOWLEDGMENTS

This research was conducted using the Cornell National Supercomputer Facility, which receives major funding from the National Science Foundation and IBM Corporation.

We thank especially Mitchell Feigenbaum and Peter Veerman for many valuable discussions. This work was supported by the National Science Foundation under grant DMS-8701050 and U.S. Department of Energy grant DE-FG05-87ER25033.

REFERENCES

1. M. J. Feigenbaum, *Los Alamos Science* **1**:4 (1980), M. J. Feigenbaum, *J. Stat. Phys.* **21**:669 (1979).
2. M. J. Feigenbaum and R. D. Kenway, The onset of chaos, in *Statistical and Particle Physics: Common Problems and Techniques* (SUSSP Publications, Edinburgh, Scotland, 1984).
3. D. Sullivan, in *Nonlinear Evolution and Chaotic Phenomena*, G. Gallavotti and P. Zweifel, eds. (Plenum Press, New York, 1988).
4. P. Collet and J.-P. Eckmann, *Iterated Maps on the Interval as Dynamical Systems* (Birkhauser, Boston, 1980).
5. M. V. Jakobson, *J. Math. Phys.* **81**:39 (1981).
6. J. D. Farmer, *Phys. Rev. Lett.* **55**:351 (1985).
7. D. K. Umberger and J. D. Farmer, *Phys. Rev. Lett.* **55**:661 (1985).
8. M. Metropolis, M. L. Stein, and P. R. Stein, *J. Combinatorial Theory (A)* **15**:25 (1973).
9. B. Derrida, A. Gervois, and Y. Pomeau, *J. Phys. A Math. Gen.* **12**:269 (1979).
10. M. J. Feigenbaum, in *Nonlinear Evolution and Chaotic Phenomena*, G. Gallavotti and P. Zweifel, eds. (Plenum Press, New York, 1988).
11. M. J. Feigenbaum, *J. Stat. Phys.* **52**:527 (1988).
12. P. Cvitanovic, in *Nonlinear Evolution and Chaotic Phenomena*, G. Gallavotti and P. Zweifel, eds. (Plenum Press, New York, 1988).